

## Evidence of Surfactant-Induced Formation of Transient Pores in Lipid Bilayers by Using Magnetic-Fluid-Loaded Liposomes

Sylviane Lesieur,<sup>\*,†</sup> Cécile Grabielle-Madelmont,<sup>†</sup> Christine Ménager,<sup>‡</sup> Valérie Cabuil,<sup>‡</sup> Delphine Dadhi,<sup>†,‡</sup> Pascale Pierrot,<sup>†,‡</sup> and Katarina Edwards<sup>§</sup>

*Equipe Physico-Chimie des Systèmes Polyphasés, CNRS UMR 8612, F-92296 Châtenay-Malabry Cedex, France, Laboratoire des Liquides Ioniques et Interfaces Chargées, CNRS UMR 7612, Université Pierre et Marie Curie, case 63, 4 place Jussieu, F-75252 Paris Cedex, France, and Department of Physical Chemistry, Uppsala University, Box 532, S-75121 Uppsala, Sweden*

Received December 23, 2002; E-mail: sylviane.lesieur@cep.u-psud.fr

Permeability of biological membranes is a key function for exchanges of matter between cells and their environment. In living systems, the chief transport mechanism of solutes across membranes is diffusion through pores or channels normally mediated by peptides and proteins.<sup>1</sup> Many other molecules also act on membrane permeability, with sometimes dramatic effects. Soluble surfactants are among the most active ones.<sup>2</sup> They are efficient enhancers of permeability and can even provoke lysis of lipid bilayers. If one considers that many metabolites and therapeutics belong to this class of compounds, it is of prime importance to understand their action mechanism.<sup>3–5</sup> Moreover, surfactants are powerful tools for solubilizing and purifying biological membrane components or for the delivery of drugs.<sup>6,7</sup>

A widely accepted strategy for modeling surfactant–membrane interactions consists of characterizing the surfactant–lipid structures produced by the progressive addition of surfactant to lipid vesicles or liposomes until surfactant–lipid mixed micelles are obtained. The present report deals with the first stage of the vesicle-to-micelle transition corresponding to sublytic surfactant concentrations. At this stage, the surfactant molecules insert into the liposome membrane without disruption. Only the permeability of the lipid bilayer is affected. Despite the accumulated evidence for permeation of high-molecular-mass solutes across the liposome membrane, one remaining challenge is to prove the formation of real holes in the lipid bilayer.<sup>4</sup> The major snag arises from the use of hydrophilic polymers as permeability markers which can unfortunately adopt variable conformations, more or less stretched, and do not necessarily require large openings to pass across a lipid bilayer.<sup>8</sup> The novelty here is to replace polymers by solid nanoparticles of definite size and shape. A reliable method is proposed for producing large unilamellar phospholipid vesicles encapsulating calibrated particles of maghemite ( $\gamma$ -Fe<sub>2</sub>O<sub>3</sub>), specially synthesized to be stable in neutral aqueous media. The leakage of the particles was induced by the action of the nonionic surfactant octyl- $\beta$ -D-glucopyranoside (OG), chosen as a model because the mechanism of phospholipid solubilization by this surfactant is one of the best documented.<sup>4,9</sup>

Monodisperse  $\gamma$ -Fe<sub>2</sub>O<sub>3</sub> nanocrystals were synthesized by oxidizing magnetite (Fe<sub>3</sub>O<sub>4</sub>, 1.3 mol) into HNO<sub>3</sub>, 2 N (1 L) containing Fe(NO<sub>3</sub>)<sub>3</sub> (1.3 mol) under boiling. After being decantation-sieved, the maghemite particles were suspended in water with 70 g of sodium citrate (NaC) before being heated at 80 °C for 30 min and precipitated in acetone at 25 °C.<sup>10</sup> Highly stable nanoparticles, negatively charged, were recovered in pH 7 water (0.63 M [Fe(III)] from flame spectrometry) and 23 mM NaC adjusted by

dialysis under conductivity controlling. The suspension behaved as a magnetic fluid composed of monodisperse superparamagnetic grains of 8 nm in diameter (Supporting Information).<sup>11</sup>

The liposomes were prepared by hydration of egg phosphatidylcholine (EPC) films in the presence of the maghemite particle suspension twice diluted with 23 mM NaC ([Fe(III)], 315 mM; [EPC], 13.7 mM) followed by sequential extrusion through polycarbonate filters of decreasing pore diameters (0.8/0.4/0.2/0.2  $\mu$ m). Nonencapsulated particles were removed by gel exclusion chromatography (GEC).<sup>12</sup> Figure 1a reports GEC profiles of unloaded EPC vesicles used as standards (peak L) and maghemite particles (peak F), injected separately. The two peaks present no overlapping. This allowed the recovery of maghemite-loaded liposomes free of external particles by collecting the sample fraction eluting in the 5–7 mL volume range (Figure 1b). The chromatography of this fraction verified the absence of contaminating external particles (Figure 1c).

The cryo-transmission electron microscopy (cryo-TEM) picture principally showed maghemite-loaded vesicles, unilamellar and spherically shaped with diameters centered around 200 nm (Figure 2a). The entrapped particles presented neither cooperative aggregation nor adhesion onto the lipid bilayers. They looked identical to those of the initial suspension with unit diameters close to the magnetic size of 8 nm (Figure 2b). Quasi-elastic light-scattering (QELS) measurements (Coulter Electronics Apparatus) confirmed the cryo-TEM analysis. Hydrodynamic diameters of 290  $\pm$  60 (liposomes) and 13  $\pm$  5 nm ( $\gamma$ -Fe<sub>2</sub>O<sub>3</sub> particles) were found, the slight excess size arising from the water layer carried by the vesicles or particles into their Brownian motion. The liposomes were stable over 6 months.

The encapsulation efficiency of the liposomes  $r_E$  is the ratio of the number of particles contained in the internal volume of the liposomes (i.e., maghemite content of the GEC-purified fraction) to the total number of particles added to the lipids before liposome formation (i.e., maghemite content of the preparation before GEC purification). Both contents were determined from the absorption spectra of maghemite at 490 nm. Total solubilization of the phospholipids into micelles ([EPC] = 1 mM) by OG ([OG] = 25 mM)<sup>9</sup> was performed before analysis to get the total release of the entrapped particles from the liposomes and to suppress parasitic scattering of light by vesicles. It resulted in a  $r_E$  of 1 Fe(III) mol % (one maghemite particle encapsulated per one hundred). This amounted to an average composition ( $r_E$ )·([Fe(III)]/[EPC]) of 0.23 mol of Fe(III) encapsulated per mol of EPC, allowing one to detect down to 0.1% particle leakage.

When surfactant is added to liposomes, it partitions between water and lipid aggregates. Each stage of the vesicle-to-micelle

<sup>†</sup> Equipe Physico-Chimie des Systèmes Polyphasés.

<sup>‡</sup> Laboratoire des Liquides Ioniques et Interfaces Chargées.

<sup>§</sup> Uppsala University.

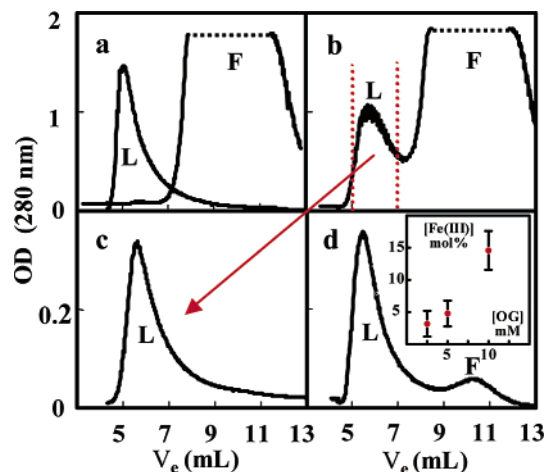


**Figure 1.** Gel exclusion chromatograms of (a) pure 300 nm EPC liposomes (20 mM EPC) and maghemite particles (300 mM Fe(III)), both injected separately; (b) mixture of EPC and maghemite particles after extrusion (13.7 mM EPC, 315 mM Fe(III)); (c) liposome fraction (2 mM EPC) collected in the 5–7 mL range (see arrow and dotted lines in (b)); and (d) maghemite-loaded liposomes (2 mM EPC) incubated in 10 mM OG for 2 h. Analyses were performed with a 1 × 11 cm Sephacryl S1000 column connected to an injection valve and a HPLC Hitachi pump (model L3000, Merck). Aqueous eluent: 23 mM NaCl (a–c) or 10 mM OG, 23 mM NaCl (d). Flow rate: 0.2 mL/min. Sample loading: 0.1 mL (a,c,d) or 0.3 mL (b). Liposomes (L) and free maghemite particles (F). Inset: released maghemite versus OG concentration; [Fe(III)] in mol % is the ratio of peak F surface area to that from liposomes fully solubilized by 25 mM OG.<sup>9</sup>

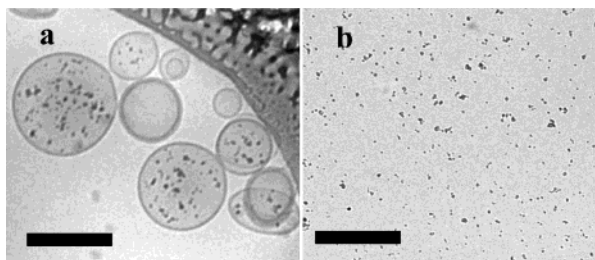


**Figure 2.** Cryo-TEM pictures of (a) maghemite-loaded liposomes and (b) maghemite particles collected at the end of the gel exclusion column. Bars = 200 nm. 10–500 nm sample films were vitrified by quick freezing in liquid ethane and transferred to a Zeiss EM 902 transmission electron microscope for examination below  $-165^{\circ}\text{C}$  (zero-loss bright-field mode, 80 kV accelerating voltage).<sup>13</sup>

transition is delimited by a given critical surfactant-to-lipid ratio in the aggregates in equilibrium with a given critical surfactant concentration in the aqueous continuum.<sup>3,4</sup> For EPC vesicles, the maximum threshold of OG molecules keeping intact the vesicle state corresponds to a 1.1 OG-to-EPC molar ratio in the aggregates and 14.3 mM OG in the aqueous medium.<sup>9</sup> To impose such sublytic conditions, the maghemite-loaded liposomes (2 mM EPC) were incubated in 2.5, 5, and 10 mM OG solutions for 2 h.<sup>14</sup> GEC analysis was then performed by using the incubation media as eluents to preserve OG partitioning. As exemplified by Figure 1d, two elution peaks were observed at the L and F positions, attributed to liposomes and free released particles, respectively, by QELS from fractions collected under each. Peak L was almost unchanged as compared to that from nonincubated liposomes (Figure 1c), QELS diameter as well. Thus, vesicle structure and concentration were not modified by OG. The absorption spectrum of fraction L showed a band at 490 nm typical of maghemite particles which were then

partly still inside the liposomes. Maghemite leakage increased with increasing OG concentration, from 3 mol % at 2.5 mM OG up to 14 mol % at 10 mM OG (Figure 1d, inset), and was time-limited.<sup>14</sup> Such a passage of solid spheres across lipid bilayers cannot be explained otherwise than by OG-catalyzed formation of pores, the diameter of which, at least, equalized that of the spheres, that is, 8 nm. Indeed, particle negative charge and preservation of both vesicle size and concentration rather ruled out any lipid-assisted mechanism, exocytosis-like, which would have modified vesicle characteristics or even destroyed a part of them, especially at 14 mol % leakage. Restricted leakage of nanospheres ascertained that the liposome membrane was only temporarily opened by OG before it definitively closed up again.

These experiments prove the ability of OG to help the transport of solid particles across lipid membranes. The temporary passage of rigid spheres, twice larger than the thickness of a phospholipid bilayer, strongly inclines toward the formation of real openings or pores by the surfactant. Such a structural evolution exemplifies the self-repair behavior of lipid assemblies which is a key function of living systems. Applicationwise, this work provides a reliable method for producing unilamellar magnetic-fluid-loaded liposomes. These tools are of interest for membrane permeability studies, but also promising for biomedical applications as biocompatible vectors of magnetic particles, regarding encapsulation rate, dimensions, and stability.<sup>15</sup>

**Supporting Information Available:**  $\gamma\text{-Fe}_2\text{O}_3$  grains magnetization curve (PDF). This material is available free of charge via the Internet at <http://pubs.acs.org>.

## References

- (1) Al-Awqati, Q. *Nat. Cell Biol.* **1999**, *1*, E201.
- (2) (a) Helenius, A.; Simons, K. *Biochim. Biophys. Acta* **1975**, *415*, 29. (b) Alonso, A.; Goni, F., Guest Eds. *Biochim. Biophys. Acta Special Issue* **2000**, *1508*, 1. (c) Koynova, R.; Tenchov, B. *Curr. Opin. Colloid Interface Sci.* **2001**, *6*, 277.
- (3) (a) Lasch, J. *Biochim. Biophys. Acta* **1995**, *1241*, 269. (b) Heerklotz, H.; Seelig, J. *Biophys. J.* **2000**, *78*, 2435.
- (4) (a) Inoue, T. In *Vesicles*; Rosoff, M., Ed.; Marcel Dekker Inc.: New York, 1996; Vol. 62, pp 151–195. (b) Lesieur, S.; Ollivon, M. In *Synthetic Surfactant Vesicles*; Uchegbu, I. F., Ed.; Harwood Academic Publishers: Amsterdam, 2000; Vol. 11, pp 49–79. (c) Ollivon, M.; Lesieur, S.; Grabielle-Madelmont, C.; Paternostre, M. *Biochim. Biophys. Acta* **2000**, *1508*, 34.
- (5) (a) Seeman, P. *Pharmacol. Rev.* **1972**, *24*, 583. (b) Lohner, K. *Chem. Phys. Lipids* **1991**, *57*, 341.
- (6) (a) Rigaud, J. L.; Pitard, B.; Levy, D. *Biochim. Biophys. Acta* **1995**, *1231*, 223. (b) Le Maire, M.; Champeil, P.; Moller, J. V. *Biochim. Biophys. Acta* **2000**, *1508*, 86.
- (7) (a) Goni, F. M.; Urbaneja, M.-A.; Alonso, A. *Liposome Technology*; CRC Press: London, 1993; pp 261–273. (b) Lasic, D. D. *Liposomes: from Physics to Applications*; Elsevier: Amsterdam, 1993. (c) Lasic, D. D. In *Vesicles*; Rosoff, M., Ed.; Marcel Dekker Inc.: New York, 1996; Vol. 62, pp 447–476.
- (8) Andrieux, K.; Lesieur, P.; Lesieur, S.; Ollivon, M.; Grabielle-Madelmont, C. *Anal. Chem.* **2002**, *74*, 5217.
- (9) Beugin, S.; Grabielle-Madelmont, C.; Paternostre, M.; Ollivon, M.; Lesieur, S. *Prog. Colloid Polym. Sci.* **1995**, *98*, 206.
- (10) Massart, R. *IEEE Trans. Magn. Mater.* **1981**, *17*, 1247.
- (11) Wihlem, C.; Gazeau, F.; Roger, J.; Pons, J. N.; Salis, M. F.; Perzynski, R.; Bacri, J. C. *Phys. Rev. E* **2002**, *65*, 031404.
- (12) Lesieur, S.; Grabielle-Madelmont, C.; Paternostre, M.; Ollivon, M. *Chem. Phys. Lipids* **1993**, *64*, 57.
- (13) Almgren, M.; Edwards, K.; Karlsson, G. *Colloids Surf., A* **2000**, *174*, 3.
- (14) Longer periods of incubation, up to 5 h, changed neither GEC peaks positions, shapes, and areas nor amounts of released particles.
- (15) (a) Halbreich, A.; Roger, J.; Pons, J.-N.; Geldwerth, D.; Da Silva, M.-F.; Roudier, M.; Bacri, J.-C. *Biochimie* **1998**, *80*, 379. (b) Tilcock, C. *Adv. Drug Delivery Rev.* **1999**, *37*, 33. (c) Roger, J.; Pons, J.-N.; Massart, R.; Halbreich, A.; Bacri, J.-C. *Eur. Phys. J. Appl. Phys.* **1999**, *5*, 321. (d) Sandre, O.; Ménager, C.; Prost, J.; Cabuil, V.; Bacri, J.-C.; Cebers, A. *Phys. Rev. E* **2000**, *62*, 3865.

JA021471J